Published for SISSA by Springer

Received: October 18, 2016
Revised: February 24, 2017
Accepted: February 28, 2017
Published: April 4, 2017

DC conductivities from non-relativistic scaling geometries with momentum dissipation

S. Cremonini,[a] **Hai-Shan Liu,**[b,c] **H. Lü**[d] **and C.N. Pope**[c,d,e]

[a] *Department of Physics, Lehigh University, 16 Memorial Drive East, Bethlehem, PA 18018, U.S.A.*

[b] *Institute for Advanced Physics & Mathematics, Zhejiang University of Technology, Hangzhou 310023, China*

[c] *George P. & Cynthia Woods Mitchell Institute for Fundamental Physics and Astronomy, Texas A&M University, College Station, TX 77843, U.S.A.*

[d] *Center for Advanced Quantum Studies, Department of Physics, Beijing Normal University, Beijing 100875, China*

[e] *DAMTP, Centre for Mathematical Sciences, Cambridge University, Wilberforce Road, Cambridge CB3 OWA, U.K.*

E-mail: cremonini@lehigh.edu, hsliu.zju@gmail.com, mrhonglu@gmail.com, pope@physics.tamu.edu

Abstract: We consider a gravitational theory with two Maxwell fields, a dilatonic scalar and spatially dependent axions. Black brane solutions to this theory are Lifshitz-like and violate hyperscaling. Working with electrically charged solutions, we calculate analytically the holographic DC conductivities when both gauge fields are allowed to fluctuate. We discuss some of the subtleties associated with relating the horizon to the boundary data, focusing on the role of Lifshitz asymptotics and the presence of multiple gauge fields. The axionic scalars lead to momentum dissipation in the dual holographic theory. Finally, we examine the behavior of the DC conductivities as a function of temperature, and comment on the cases in which one can obtain a linear resistivity.

Keywords: Gauge-gravity correspondence, Holography and condensed matter physics (AdS/CMT)

ArXiv ePrint: 1608.04394

doi:10.1007/JHEP04(2017)009

JHEP04(2017)009

Contents

1 Introduction

Recent years have seen an increasing interest in applying the techniques of holography to probe the rich structure of strongly coupled quantum phases of matter, and in particular their dynamics (see e.g. [1–3] for reviews in the context of condensed matter applications). Efforts are underway to model the transport properties of a variety of systems that exhibit unconventional behavior — with high temperature superconductors offering a prime example — and typically lack a well-defined quasiparticle description, due to their strongly interacting nature. As part of this program, the breaking of translational invariance (as a mechanism to dissipate momentum [4–7]) has been recognized as a crucial ingredient for a realistic description of materials with impurities and an underlying lattice structure (see e.g. [8–19]).

Indeed, when translational invariance is preserved charges are unable to dissipate their momentum, and in the presence of non-zero charge density one encounters a delta function in the AC conductivity at zero frequency, and a resulting infinite DC conductivity. Lattice effects and broken translational symmetry have been modeled holographically in a variety of ways. These include constructions involving periodic potentials and inhomogeneous lattices [9–14], realizations of homogeneous lattices [15–17] and theories without diffeomorphism invariance [18–20] — where the list is by no means exhaustive. The constructions that retain homogeneity involve ordinary (as opposed to partial) differential equations and

JHEP04(2017)009

are therefore of a clear technical advantage, as they lead to remarkable simplifications in the analysis.

Driven by the desire to model phases with anomalous scalings, there has been interest in working with geometries that violate hyperscaling — describing an anomalous scaling of the free energy parametrized by θ — and/or exhibit non-relativistic Lifshitz scaling, characterized by a dynamical critical exponent z. Among the models that maintain homogeneity, conductivity studies for these classes of geometries have appeared in [21–24], with [22] focusing on solutions that are asymptotically AdS.

In this paper, we extend these constructions by examining analytical black brane backgrounds that are Lifshitz-like and hyperscaling violating (at all energy scales), and incorporate the breaking of translational invariance along the boundary directions by appropriately adding axionic fields. The theories we consider involve two gauge fields. One is responsible for the Lifshitz-like nature of the background solutions, while the other is analogous to a standard Maxwell field in asymptotically-AdS charged black holes. Thus, the two vector fields play very different roles in the construction and in the interpretation of the physics. The solutions we work with are described in section 2 (and their generalizations in appendix A). Following the horizon method proposed by [25–28], in section 3 we compute analytically the matrix that encodes the behavior of the DC conductivity in the system. As we shall see, subtleties arise by taking into account the fluctuations of both fields.

Since our conductivity analysis relies on a horizon computation, it also applies to geometries that are Lifshitz and hyperscaling violating in the IR, but approach AdS in the UV.[1] Indeed, our results complement the related work of [22, 29], which considered $\{z, \theta\}$ scaling geometries with AdS UV completions. In particular, in the appropriate single charge limit, our results provide a concrete realization of one of the IR behaviors seen in [22]. In section 4 we comment on the different physical interpretation of the matrix of conductivities in the asymptotically Lifshitz vs. AdS case, for specific examples. A more detailed analysis of this question will be put forth in [36, 37].

Finally, in section 4 we shift our attention to the behavior of the DC conductivities as a function of temperature, restricting ourselves for simplicity to the regimes that can be treated analytically. The detailed temperature dependence of holographic conductivities has received particular attention in the light of the potential applications to the anomalous "strange metal" regime of the high temperature cuprate superconductors. A robust feature of the latter is the linear scaling of the resistivity with temperature, $\rho \sim T$. With this in mind, we examine the possible temperature behaviors allowed by our model, and identify some of the parameter choices that can lead to a linear resistivity, for both Lifshitz and AdS asymptotics. While this analysis is by no means exhaustive, it does show that there is a rich structure of possible temperature behaviors, which include in many instances the desired linear resistivity regime. As a concrete example, when the charge of the second vector field vanishes and the $\{z, \theta\}$ geometries are assumed to be asymptotic to AdS, we

[1] Clearly, to explicitly construct these geometries the scalar potential of our theory would need to be appropriately modified, to include terms that would stabilize the dilatonic scalar in the UV. While this does not pose any conceptual problem, by doing so we would lose the advantage of working with large classes of analytical solutions.

JHEP04(2017)009

identify several cases with $\rho \sim T$ (interestingly, many of them associated with $z = 4/3$). We find a more intricate temperature behavior when both charges are turned on and the asymptotics are Lifshitz, again with the existence of a linear regime for appropriate values of z and θ.

We have also examined the structure of the perturbations at the boundary, without however taking into account holographic renormalization. Still, this analysis provides intuition for how the asymptotic and horizon data are related to each other in the case of Lifshitz asymptotics, and helps shed some light on the role of boundary conditions and on the subtleties associated with working within a non-relativistic theory. This discussion is relegated to appendix B.

While we were in the final stages of this work, the related article [24] appeared, in which the authors considered the same model studied here. However, the analysis of [24] only takes into account the fluctuations of one gauge field. As we shall explain in detail in the main text, this is not a consistent truncation of the perturbation equations — consistency requires both gauge fields to fluctuate. This explains the partial discrepancy between our results and those of [24].

2 Lifshitz black holes with hyperscaling violation

In this section, we shall consider a particular case amongst the class of theories described in appendix A, in which we specialise to four-dimensional gravity coupled to two Maxwell fields, a dilaton and two axions. The Lagrangian is given by

$$e^{-1}\mathcal{L} = R - \frac{1}{2}(\partial\phi)^2 - 2\Lambda e^{\lambda_0\phi} - \frac{1}{4}e^{\lambda_1\phi}F_1^2 - \frac{1}{4}e^{\lambda_2\phi}F_2^2 - \frac{1}{2}e^{\lambda_3\phi}\big((\partial\chi_1)^2 + (\partial\chi_2)^2\big)\,. \tag{2.1}$$

The equations of motion following from this Lagrangian are

$$\begin{aligned}
R_{\mu\nu} &= \frac{1}{2}\partial_\mu\phi\,\partial_\nu\phi + \frac{1}{2}e^{\lambda_3\phi}\left(\partial_\mu\chi_1\,\partial_\nu\chi_1 + \partial_\mu\chi_2\partial_\nu\chi_2\right) + \Lambda\, e^{\lambda_0\phi}\, g_{\mu\nu} \\
&\quad + \frac{1}{2}e^{\lambda_1\phi}\left(F_{1\,\mu\rho}\,F_{1\,\nu}{}^{\rho} - \frac{1}{4}F_1^2\, g_{\mu\nu}\right) + \frac{1}{2}e^{\lambda_2\phi}\left(F_{2\,\mu\rho}\,F_{2\,\nu}{}^{\rho} - \frac{1}{4}F_2^2\, g_{\mu\nu}\right), \\
\Box\phi &= \frac{1}{2}\lambda_3\left((\partial\chi_1)^2 + (\partial\chi_2)^2\right) + \frac{1}{4}\lambda_1\, e^{\lambda_1\phi}\, F_1^2 + \frac{1}{4}\lambda_2\, e^{\lambda_2\phi}\, F_2^2 + 2\lambda_0\,\Lambda\, e^{\lambda_0\phi}\,, \\
\nabla_\mu\big(e^{\lambda_3\phi}\,\nabla^\mu\chi_1\big) &= 0\,, \qquad\qquad \nabla_\mu\big(e^{\lambda_3\phi}\,\nabla^\mu\chi_2\big) = 0\,, \\
\nabla_\mu\big(e^{\lambda_1\phi}\,F_1^{\mu\nu}\big) &= 0\,, \qquad\qquad \nabla_\mu\big(e^{\lambda_2\phi}\,F_2^{\mu\nu}\big) = 0\,.
\end{aligned} \tag{2.2}$$

The theory described by (2.1) admits Lifshitz-like, hyperscaling violating black brane solutions, given by[2]

$$\begin{aligned}
ds^2 &= r^\theta\Big(-r^{2z}f dt^2 + \frac{dr^2}{r^2 f} + r^2(dx^2+dy^2)\Big)\,, \\
\phi &= \gamma\log r\,, \qquad (A_1)_0' = Q_1\, r^{z-3-\lambda_1\gamma}\,, \qquad (A_2)_0' = Q_2\, r^{z-3-\lambda_2\gamma}\,, \\
\chi_1 &= \alpha x\,, \qquad\qquad \chi_2 = \alpha y\,,
\end{aligned} \tag{2.3}$$

[2]Our sign convention for θ is the opposite of the one commonly used in the literature.

JHEP04(2017)009

and parametrized by

$$\gamma = \sqrt{(\theta+2)(\theta+2z-2)}\,, \qquad \lambda_0 = -\frac{\theta}{\gamma}\,, \qquad \lambda_1 = -\frac{(4+\theta)}{\gamma}\,,$$
$$\lambda_2 = \frac{(\theta+2z-2)}{\gamma}\,, \qquad \lambda_3 = -\frac{\gamma}{\theta+2}\,, \qquad Q_1 = \sqrt{2(z-1)(\theta+z+2)}\,,$$
$$\Lambda = -\frac{1}{2}(\theta+z+1)(\theta+z+2) \qquad . \tag{2.4}$$

Note that the logarithmically-running scalar ϕ breaks the exact Lifshitz symmetry of the metric. The blackening function f takes the form

$$f = 1 - \frac{m}{r^{\theta+z+2}} + \frac{Q_2^2}{2(\theta+2)(\theta+z)\,r^{2(\theta+z+1)}} + \frac{\alpha^2}{(\theta+2)(z-2)\,r^{\theta+2z}}\,, \tag{2.5}$$

with m the integration constant denoting the mass parameter. The solution is divergent when $z = 2$, indicating logarithmic behavior. Indeed, when $z = 2$, the solution becomes

$$f = 1 - \frac{1}{r^{\theta+4}}\left(m + \frac{\alpha^2}{\theta+2}\log r\right) + \frac{Q_2^2}{2(\theta+2)^2 r^{2(\theta+3)}}\,. \tag{2.6}$$

Thus the α term contributes a logarithmic divergence to the mass.

For fixed z, the solution contains three free integration constants, m, α and Q_2. The solution reduces to the Lifshitz-like vacuum when these parameters vanish. In this paper, we are not only considering the IR region near the black hole horizon, but the entire black hole solution (2.3) including its asymptotic properties at infinity. In order for the vacuum to avoid a curvature singularity at the asymptotic boundary $r = \infty$, we must require[3]

$$\theta \geq 0\,. \tag{2.7}$$

We must also require

$$(2+\theta)(2z-2+\theta) \geq 0\,, \qquad (z-1)(2+z+\theta) \geq 0\,, \tag{2.8}$$

in order to ensure that γ and Q_1 are real. These last two conditions are in fact equivalent to the requirement that the null energy condition be satisfied. Thus, since z must necessarily be positive, we must have $z \geq 1$. This, together with (2.7), implies $f(\infty) = 1$. Thus the solution is asymptotically Lifshitz-like with hyperscaling violation. In fact the solution (2.3) describes a charged black hole whose Hawking temperature is

$$T = \frac{r_0^{z+1}\, f'(r_0)}{4\pi}\,, \tag{2.9}$$

where r_0 is the radius of the horizon, located at the largest root of $f(r) = 0$.

It should be noted that the two Maxwell fields play very different roles in the black hole solution. The field A_1 is responsible for the Lifshitz-like nature of the vacuum. In

[3]If one treats the solution (2.3) as merely an approximation to the geometry in the IR region, and assumes instead AdS asymptotics, this condition can be relaxed and negative values of θ are allowed.

JHEP04(2017)009

particular, its "charge" Q_1 is fixed, for given Lifshitz and hyperscaling violating exponents z and θ, and the solution becomes asymptotically AdS if $Q_1 = 0$. By contrast, the charge Q_2 of the field A_2 is a freely-specifiable parameter, analogous to the electric charge of a Reissner-Nordström black hole. We will come back to this point when we discuss the physical interpretation of our results for different asymptotics.

For reasons that will become apparent shortly, and to make contact with some of the literature, we would like to parametrize the scalings of the two gauge fields in terms of two exponents ζ_1 and ζ_2, the analogs of the conduction exponent ζ that controls the anomalous scaling dimension of the charge density operator [31–33]. Letting[4] $\zeta_1 = -2-\theta$, the scaling of the A_1 gauge field is then of the form

$$A_1 \sim r^{z-\zeta_1} dt\,. \tag{2.10}$$

Similarly, introducing $\zeta_2 = 2z+\theta$, the second gauge field can be written as

$$A_2 \sim r^{z-\zeta_2} dt\,. \tag{2.11}$$

3 DC conductivity from horizon data

By now there are several techniques available for computing holographic DC conductivities. Using Kubo's formula, the optical conductivity can be extracted from the current-current propagator in the boundary,

$$\sigma^{ij}(\omega) = \frac{\partial}{\partial E_j(\omega)} \langle J^i(\omega)\rangle = -\frac{1}{\mathrm{i}\omega} \langle J^i(\omega) J^j(\omega)\rangle\,, \tag{3.1}$$

with the current found by varying the action with respect to the external source, i.e. schematically $\langle J(\omega)\rangle = \frac{\partial S}{\partial A_{\rm ext}(\omega)}$. The DC conductivity is then simply the zero frequency limit of the optical conductivity,

$$\sigma^{ij}_{\rm DC} = \lim_{\omega\to 0} \sigma^{ij}(\omega)\,. \tag{3.2}$$

A great simplification in these calculations comes from the membrane paradigm approach of [34], i.e. the realization that the currents in the boundary theory can be identified with radially independent quantities in the bulk. In the presence of momentum dissipation, the method of [34] was first extended by [20], who noted that one can generically identify — in the zero frequency limit — a massless mode that does not evolve between the horizon and the boundary. A much more general understanding of this behavior, and in particular of the universality of the equivalence between horizon and boundary current fluxes, was later obtained in [25–28]. Moreover, it was shown [26–28] that the field theory thermoelectric DC conductivity can be found by solving generalized Stokes equations on the black hole horizon.

The general procedure for computing DC conductivities entails studying time-dependent perturbations of the relevant fields. In particular, one typically turns on an oscillating

[4] Note that $\zeta_1 = -d_\theta$, where $d_\theta \equiv 2+\theta$ is the effective dimensionality factor in four space-time dimensions.

JHEP04(2017)009

electric field with frequency ω, computes the response and then takes the $\omega \to 0$ limit to extract $\sigma_{\rm DC}$. However, in the newer approach developed by [25], instead of taking the zero-frequency limit of the optical conductivity, one switches on a constant electric field from the start[5], and then computes the response. In this section we will adopt the horizon approach of [25–28]. Appendix B includes an asymptotic analysis of the behavior of the fluctuations, which offers an alternative way to compute the matrix of conductivities.

Following the ansatz of [25], we therefore consider the perturbations[6]

$$(\delta A_i)_x = -E_i t + a_i(r)\,, \qquad \delta g_{tx} = r^{\theta+2}\,\psi(r)\,, \qquad \delta\chi_1 = b(r)\,. \tag{3.3}$$

Substituting them into the equations of motion (2.2), we see that the two Maxwell equations imply $j_1' = 0$ and $j_2' = 0$, where

$$j_1 = -\big(Q_1\psi + r^{z-3-\theta} f a_1'\big)\,, \qquad j_2 = -\big(Q_2\psi + r^{3z-1+\theta} f a_2'\big)\,. \tag{3.4}$$

Thus j_1 and j_2 are constants of integration. They of course describe precisely the two conserved currents in the system. Similarly, the axion equations imply $j_0' = 0$, where

$$j_0 = r^{5-z} f\, b'\,, \tag{3.5}$$

and hence j_0 is another constant of integration. The Einstein equations then imply

$$E_1 Q_1 + E_2 Q_2 = j_0 \alpha\,, \tag{3.6}$$

and

$$\Big(r^{5-z+\theta}\,\psi' + Q_1 a_1 + Q_2 a_2\Big)' = \frac{\alpha^2}{r^{3z-3}\,f}\,\psi\,. \tag{3.7}$$

Using (3.4), this becomes

$$f\,(r^{5-z+\theta}\psi')' = \frac{1}{r^{3z-1+\theta}}\Big[\Big(Q_2^2 + r^{2+\theta}(\alpha^2 + Q_1^2 r^{(2z+\theta)})\Big)\,\psi + j_2 Q_2 + j_1 Q_1 r^{2(z+1+\theta)}\Big]\,. \tag{3.8}$$

Finally, the dilaton equation gives no contribution at linear order in perturbations.

As we mentioned earlier, the field A_2 is analogous to a standard Maxwell field in an asymptotically AdS charged black hole, whereas the field A_1 is responsible for modifying the vacuum to become Lifshitz-like. It is thus tempting to think that one could consider perturbations around the background in which only A_2, but not A_1, is allowed to fluctuate. In fact, this is what was done in references [24, 35]. However, a truncation where the perturbation of a_1 is set to zero is inconsistent[7] with the full set of equations of motion. In our discussion, we shall therefore take a_1, as well as a_2, to be non-vanishing.

[5] This amounts to just considering the first two terms in the Taylor expansion of $e^{-i\omega t}$. In fact, the only terms where linear t dependence arises are in the perturbations of the gauge field potentials. The associated static electric fields are described in terms of gauge potentials that depend linearly on t.

[6] Note that in the literature, a δg_{rx} perturbation is sometimes included. This, however, is pure gauge, and can be removed by an appropriate coordinate transformation $x \to x + \beta(r)$, together with a corresponding field redefinition of $b(r)$.

[7] As can be seen from eqns (3.4), turning off the perturbation a_1 forces ψ to be a constant, which from (3.8) implies that $j_1 Q_2 = j_2 Q_1$ and (if $\alpha^2 \neq 0$) that $j_1 = 0$. In all cases, the equation for a_2 in (3.4) then implies that a_2 is a constant, which means it is pure gauge.

JHEP04(2017)009

The two leading-order terms in the large-r expansion of ψ at large r can be seen, from (3.8), to be of the form

$$\psi = -\frac{j_1}{Q_1} + \frac{\beta_1}{r^{z+2+\theta}} + \beta_2\, r^{2z-2} + \cdots . \tag{3.9}$$

We must take $\beta_2 = 0$ for regularity, and hence at the boundary we have $\psi_\infty \equiv \psi(\infty) = -\frac{j_1}{Q_1}$. On the other hand evaluating (3.8) on the horizon implies that

$$\psi_0 \equiv \psi(r_0) = -\frac{j_2\, Q_2 + j_1\, Q_1\, r_0^{2(z+1+\theta)}}{Q_2^2 + (\alpha^2 + Q_1^2\, r_0^{2z+\theta})\, r_0^{2+\theta}} . \tag{3.10}$$

Now, it follows from (3.3) that in order for the perturbations $(\delta A_i)_x$ to be purely ingoing on the horizon, we must have $a_i \sim -E_i\, r_*$ near the horizon, where the tortoise coordinate r_* is defined by $dr_* = dr/(r^{z+1}\, f(r))$. Thus near the horizon we must have $a_i' = -\frac{E_i}{r^{z+1}\, f(r)} + \cdots$ and so, from (3.4), we have

$$j_1 = -Q_1\psi_0 + \frac{E_1}{r_0^{4+\theta}} , \qquad j_2 = -Q_2\psi_0 + E_2 r_0^{2z-2+\theta} . \tag{3.11}$$

Finally, combining these with (3.10) and expressing j_1, j_2 entirely in terms of E_1 and E_2, in analogy with Ohm's law, we find the following matrix-valued equation for the currents,

$$\begin{pmatrix} j_1 \\ j_2 \end{pmatrix} = \begin{pmatrix} \sigma_{11} & \sigma_{12} \\ \sigma_{21} & \sigma_{22} \end{pmatrix} \begin{pmatrix} E_1 \\ E_2 \end{pmatrix} , \tag{3.12}$$

with the entries of the conductivity matrix given by

$$\begin{aligned} \sigma_{11} &= \frac{1}{r_0^{4+\theta}} + \frac{Q_1^2\, r_0^{2z-4}}{\alpha^2} , \qquad \sigma_{12} = \frac{Q_1 Q_2 r_0^{2z-4}}{\alpha^2} , \\ \sigma_{21} &= \sigma_{12} , \qquad \sigma_{22} = r_0^{2z-2+\theta} + \frac{Q_2^2}{\alpha^2} r_0^{2z-4} . \end{aligned} \tag{3.13}$$

Recall, however, that here the two currents j_1 and j_2 are associated with two distinct vector fields, which are oriented along the same spatial direction. Thus, the coefficients appearing in the matrix σ_{ij} should not be confused with those associated with different space-time directions.

It is also worth noting that in the limit $z \to 1$ and $\theta \to 0$, for which $Q_1 \to 0$, the quantity σ_{11} goes to r_0^{-4}. On the other hand, if we had set $Q_1 = 0$ from the outset, the solution would have been simply the Schwarzschild-AdS black hole, and hence we would have $\sigma_{11} = 1$. Thus we have a discontinuity in the $Q_1 \to 0$ limit. This discontinuity can be understood from the fact that turning on Q_1 changes the asymptotic structure from an AdS to a Lifshitz like one. No matter how small Q_1 is, the perturbation $(\delta A_1)_x$ of the associated gauge potential must be even smaller. Thus the perturbation we are considering here would actually vanish in the $Q_1 \to 0$ limit, and so it could not possibly have a continuous limit to the perturbation that is normally considered in the $Q_1 = 0$ Schwarzschild-AdS background. This provides one explanation for why the dependence

JHEP04(2017)009

of the conductivity on the temperature is different from that in the RN black hole. We come back to the issue of the different physical interpretations of the two currents in the discussion below. In closing, we should note that although σ_{22} above naively agrees with the result of [24], the latter did not take into account both gauge field fluctuations. Indeed, setting $Q_1 = 0$ in the equations above is *not* consistent with the linearized fluctuation equations unless one also sets $z = 1$.

4 Interpreting the matrix of conductivities — AdS vs. Lifshitz

The matrix (3.13) encodes in a non-trivial way the conductive response to the presence of two U(1) fields, in a system that in general is non-relativistic. Its interpretation is subtle, and depends on the particular form of the asymptotics of the solution as well as the value of the charges. Relativistic symmetry in this theory is recovered when $Q_1 = 0$, which corresponds to $z = 1$. While here we provide only a preliminary discussion of the physics of (3.13), a more detailed analysis is relegated to [36, 37].

A point we would like to emphasize is that the horizon analysis of the previous section also applies to black hole solutions that are only non-relativistic in the far IR, and become relativistic in the UV by approaching AdS asymptotically. While geometries with AdS asymptotics are *not* exact solutions to our action as it stands, they can be easily generated by making minor modifications to the scalar potential which would only affect the UV properties of the solutions, leaving their near-horizon behavior unchanged.[8] For this reason, we claim that it is still valuable to inspect the behavior of σ_{ij} even assuming standard, relativistic (AdS) boundary conditions, as well as for the case we are focusing on, in which the boundary is Lifshitz and hyperscaling violating.

In this discussion we are going to focus on two cases, postponing further clarifications to [36, 37]. First, we shall examine the single charge case $Q_2 = 0$. Next, we will restore Q_2 and consider instead $j_1 = 0$:

1. When $Q_2 = 0$ one can truncate out the gauge field A_2 from the theory. The σ_{ij} matrix in (3.12) then becomes diagonal, and the conductivity associated with the remaining U(1) field A_1 is simply σ_{11}. The physical interpretation of the σ_{11} component depends on whether the asymptotics are Lifshitz [47–49], as in the explicit solutions used in this paper, or AdS:

   - For Lifshitz asymptotics the current associated with A_1 has the interpretation of an energy flux, in the approach of [47, 48], or a mass current in that of [49]. In either formalism, σ_{11} does *not* represent the DC conductivity in the system. One sign of the peculiarity of this example is that the charge Q_1 is not a free parameter in the theory, but instead is fixed by z. Thus, the single charge case $Q_2 = 0$ for asymptotically Lifshitz geometries does not encode information about electrical conductivities, and we will not comment on it further.
   - If the near-horizon solutions studied here were embedded in a theory that allowed for AdS asymptotics, j_1 would be a genuine electrical current, and σ_{11} would

[8] That this can indeed be done has been shown explicitly in a number of examples in the literature.

JHEP04(2017)009

indeed be identified with the DC conductivity, $\sigma^{\rm DC} = \sigma_{11}$. Written in terms of the scalar couplings appearing in the Lagrangian, we have

$$\sigma^{\rm DC} = e^{\lambda_1 \phi_0} + \frac{Q_1^2}{\alpha^2\, r_0^{2+\theta}}\, e^{-\lambda_3 \phi_0}\,. \tag{4.1}$$

In this form it is apparent that the coupling between the axionic fields and the dilatonic scalar is responsible for generating temperature dependent terms which are sensitive to the mechanism to relax momentum. In particular, as we shall see in section 4, the term proportional to Q_1^2/α^2 can give a temperature dependence of the form $\sim T^{-1}$, and therefore a linear behavior for the resistivity. Finally, we should note that (4.1) is precisely of the form found in [22], whose setup falls within the class of models we are discussing when $Q_2 = 0$.

2. Next, we examine the special case for which $j_1 = 0$, in which the conductivity matrix simplifies significantly, yet the system still displays a rich behavior. Note that having $j_1 = 0$ does *not* mean that the fluctuation $\delta(A_1)_x$ is turned off. On the other hand, it corresponds to the situation in which the sources E_1 and E_2 can not be turned on independently,[9] but rather are related via

$$\sigma_{11} E_1 + \sigma_{12} E_2 = 0\,. \tag{4.2}$$

We can use (3.12) with $j_1 = 0$ to trade E_1 for E_2, and extract the DC conductivity by reorganizing the resulting expression for the remaining current, $j_2 = \sigma_2^{\rm DC}\, E_2$. We find

$$\sigma_2^{\rm DC} = r_0^{2z-2+\theta} \left[1 + \frac{Q_2^2}{r_0^{2+\theta}(\alpha^2 + Q_1^2\, r_0^{2z+\theta})}\right]. \tag{4.3}$$

We emphasize that this is *not* the same as the original σ_{22}. Indeed, this expression is sensitive to the presence of both charges. In particular, the contribution from Q_1 introduces additional temperature dependence, which is absent in σ_{22} and would also not be present in the single charge case above (for which $Q_2 = 0$). This additional dependence was also missed by [24], as we emphasized earlier.

Recall that when $Q_1 = 0$ we lose the Lifshitz scaling of the background ($z = 1$). When both charges vanish, the DC conductivity (4.3) becomes

$$\sigma_2^{\rm DC} = r_0^{\theta}\,, \tag{4.4}$$

corresponding to a geometry that is conformal to AdS, and reduces to the well-known result of [40], $\sigma_2^{\rm DC} = 1$, when the background respects hyperscaling, $\theta = 0$. Thus we see that the gauge field A_2 and its charge Q_2 can be viewed as generalizations of the gauge

[9] A preliminary asymptotic analysis seems to indicate that in the range $1 \leq z \leq \frac{4}{3}$ only the linear combination of E_1 and E_2 which doesn't source j_1 can be turned on while keeping the geometry regular. We refer the reader to appendix B for further details, but stress that a proper asymptotic analysis should take into account holographic renormalization.

JHEP04(2017)009

field in the Reissner-Nordström black hole. To examine the structure of the conductivity matrix more generally, one needs to have a better understanding of how to extract sources and VEVs in the case of Lifshitz and hyperscaling violating asymptotics, in the presence of momentum dissipation [36].

Finally, it is worth remarking that the conductivities we obtained in this section were solely obtained from the horizon data. The requirement that the perturbations be well behaved at infinity may give further constraints on the parameters in the solution. Since the solutions (2.3) we are considering allow us to study the perturbations in the entire region exterior to the black hole, we have indeed obtained such constraints from inspecting the asymptotic behaviour of the fluctuations. This analysis is relegated to appendix B.

5 Temperature dependence

We are now ready to discuss the issue of the temperature dependence of the conductivities. Our main interest is in identifying parameter choices for which one can find a linear regime for the resistivity, $\rho(T) \sim T$. More generally, we want to display the rich structure of temperature behaviors that are available in these systems, in the presence of two charges. In terms of the horizon radius r_0 and the parameters α and Q_2, the Hawking temperature (2.9) is given by

$$T = \frac{z+2+\theta}{4\pi} r_0^z - \frac{Q_2^2}{8\pi(2+\theta)} \frac{1}{r_0^{z+2+2\theta}} - \frac{\alpha^2}{4\pi(2+\theta)} \frac{1}{r_0^{z+\theta}} \,. \tag{5.1}$$

When $r_0^{2z+\theta} \gg \alpha^2$ and $r_0^{2z+2+2\theta} \gg Q_2^2$, we recover the well known Lifshitz scaling

$$T \sim r_0^z \,. \tag{5.2}$$

Thus, this approximation corresponds to "large temperatures," in the sense of[10]

$$T \gg \alpha^{\frac{2z}{2z+\theta}} \quad \text{and} \quad T \gg Q_2^{\frac{z}{z+1+\theta}} \,. \tag{5.3}$$

As the temperature is lowered sufficiently, the α^2 term in (5.1), which always dominates over the Q_2^2 term provided that $\theta > -2$, has to be taken into account. The simple scaling (5.2) is then modified to[11]

$$T \sim \frac{z+2+\theta}{4\pi} r_0^z - \frac{\alpha^2}{4\pi(2+\theta)} \frac{1}{r_0^{z+\theta}} \,, \tag{5.4}$$

and can be inverted (in the large temperature, or small α limit) to obtain an expansion for r_0 as a function of T,

$$r_0 = \left(\frac{4\pi T}{z+2+\theta}\right)^{\frac{1}{z}} + \frac{\alpha^2}{4\pi z(2+\theta)} \frac{1}{T} \left(\frac{z+2+\theta}{4\pi T}\right)^{1+\frac{\theta-1}{z}} + \cdots \,. \tag{5.5}$$

We shall return to the opposite, low temperature regime at the end of this section.

[10] Note that the temperatures satisfying these ranges can be decreased/increased by tuning α and Q_2.

[11] This holds under the condition $\alpha^2 T^{\frac{2+\theta}{z}} \gg Q_2^2$, and is clearly exact when $Q_2 = 0$.

JHEP04(2017)009

Using the large T approximation (5.5), the conductivity matrix σ_{ij} given in (3.13) becomes

$$\begin{aligned}
\sigma_{11} &\sim \frac{Q_1^2}{\alpha^2}\, T^{\frac{2z-4}{z}} + T^{-\frac{(4+\theta)}{z}} + \dots\,, \\
\sigma_{12} &\sim Q_1 Q_2 \left(\frac{1}{\alpha^2}\, T^{\frac{2z-4}{z}} + (z-2)\, T^{-\frac{(4+\theta)}{z}} \right) + \dots\,, \\
\sigma_{22} &\sim T^{\frac{2z-2+\theta}{z}} + \frac{Q_2^2}{\alpha^2}\, T^{\frac{2z-4}{z}} + Q_2^2\,(z-2)\, T^{-\frac{(4+\theta)}{z}} + \dots\,,
\end{aligned} \tag{5.6}$$

where each term in each component is smaller than the preceding one (we dropped all strictly positive numerical factors that don't involve the parameters $\{Q_1, Q_2, \alpha\}$). In order to understand the temperature behavior over a wider range one must invert (5.1) for generic values of the scaling exponents. Finally, note that while the Q_1 charge naively sets a scale that is different from those controlling the temperature, which are Q_2 and α, it is fully determined by the background, i.e. it is fixed in terms of z and θ, as given in (2.4). Next, we are now going to examine the same two cases that were singled out in section 4.

5.1 Single charge case ($Q_2 = 0$), AdS asymptotics

Recall that when $Q_2 = 0$ the conductivity matrix σ_{ij} reduces to σ_{11}. We explained in section 4 that for Lifshitz asymptotics the component σ_{11} does not represent the electrical DC conductivity in the system. Thus, we will discuss instead its behavior assuming that the solutions can be embedded in AdS. This can be achieved by slightly modifying the model, in the manner described in section 4, and without affecting the horizon properties of the geometry. One then has the usual interpretation $\sigma_{DC} = \sigma_{11}$.

Written in terms of the conduction exponent $\zeta_1 = -2-\theta$ defined in (2.10) and the parameters (2.4) describing our solution, the temperature dependence of the DC conductivity read off from (5.6) is then

$$\sigma_{DC} \sim T^{\frac{\zeta_1-2}{z}} + \frac{Q_1^2}{\alpha^2}\, T^{\frac{\zeta_1-\lambda_3\gamma}{z}} + \dots \;=\; T^{\frac{\zeta_1-2}{z}} \left(1 + \frac{Q_1^2}{\alpha^2}\, T^{\frac{2z+\theta}{z}} \right) + \dots\,. \tag{5.7}$$

The two terms in this expression generically compete with each other. However, when the "large temperature" condition (5.3) holds, the first term dominates[12] for $(2z+\theta)/z < 0$, while the second one is the dominant one when $(2z+\theta)/z > 0$. We emphasize that negative values of θ are allowed for AdS asymptotics (while they are excluded in the asymptotically Lifshitz case to avoid curvature singularities in the UV).

We have inspected (5.7) more carefully in a number of cases of particular interest. We focus on the ones that allow for $\sigma_{DC} \sim T^{-1}$, so that the resistivity scales like $\rho \sim T$:

- When $z = 4+\theta$ and $-4 < \theta < -8/3$ the first term $\sim T^{\frac{\zeta_1-2}{z}}$ dominates, yielding the scaling $\sigma_{DC} \sim T^{-1}$ in the regime (5.3).
- Again in the regime (5.3), the choice $z = 4/3$ yields

$$\sigma_{DC} \sim \frac{Q_1^2}{\alpha^2}\,\frac{1}{T} + \frac{1}{T^{3+3\theta/4}} \quad \Rightarrow \quad \rho \sim \frac{T^{3+\frac{3\theta}{4}}}{1 + \frac{Q_1^2}{\alpha^2} T^{2+\frac{3\theta}{4}}}\,. \tag{5.8}$$

At leading order and assuming $\theta > 0$, this is associated with a linear resistivity $\rho \sim T$.

[12] Since $Q_1 \sim \mathcal{O}(1)$, it doesn't affect this argument.

JHEP04(2017)009

- When $\theta = -2z$ the relation (5.1) yields the exact expression

$$T = \left[\frac{z+2+\theta}{4\pi} - \frac{\alpha^2}{4\pi(2+\theta)}\right] r_0^z \,, \tag{5.9}$$

  and the temperature scaling is precisely $T \sim r_0^z$. Indeed in this case the conductivity scales as $T^{2-\frac{4}{z}}$, and when $z = 4/3$ and $\theta = -8/3$ one has $\sigma_{\rm DC} \sim T^{-1}$ and $\rho \sim T$.

- Another interesting choice is that of $z = 4/3$ and $\theta = -z$, which yields

$$\sigma_1^{\rm DC} \sim \frac{\alpha^2 + Q_1^2 T}{\alpha^2 T^2} \,, \tag{5.10}$$

  and therefore a quadratic regime for the resistivity below the linear one.

In full generality one should solve for the temperature dependence numerically, since subleading effects will become crucial when going to even smaller temperatures.

Intriguingly, the cases with $z = 4/3$ are partially reminiscent of that singled out by [41], whose analysis relied on purely field-theoretic arguments. Naively, the set of values identified by [41], $z = 4/3, \theta = 0$ and $\Phi = -2/3$ (with Φ related to the conduction exponent in the theory) are not consistent with each other in our model.[13] One should keep in mind, however, that a direct comparison between our model and the setup of [41] can be quite subtle. In particular, the identification of the conduction exponent in our setup depends on the asymptotics and on the physical interpretation of each vector field.

Still, we find it interesting that the linear resistivity regimes which arise from the Q_1^2/α^2 terms in (5.7) are all associated with $z = 4/3$. This value also plays a special role in the asymptotic analysis in the case of Lifshitz asymptotics, as discussed in appendix B. That the choices $\{z = 4/3,\ \theta = -8/3\}$ as well as $\{z = 4/3,\ \theta = -4/3\}$ are allowed by all energy and stability conditions, provided one has AdS asymptotics, can be seen from the parameter ranges summarized e.g. in [42]. Finally, we note that (5.7) matches[14] the generic behavior observed in [22]. More specifically, when $z > 1$ our expression for σ_{11} falls into Class III of [22], with our near-horizon solutions providing an explicit example of the type of behavior considered there.

5.2 $j_1 = 0$ case

We now return to the case of Lifshitz asymptotics, and examine the special choice $j_1 = 0$, for which the two sources E_1, E_2 are not independent of each other, but rather obey (4.2). Examining the structure of $\sigma_2^{\rm DC}$ given by (4.3), we find a rich behavior for σ_{DC}, depending on the range of temperature and the choice of scaling exponents, as well as the interplay between the strength α of the axionic sources and the tunable charge Q_2. In particular, recall that the exponents z and θ are constrained by the conditions described in section 2.

Below we examine a few representative cases, again with a focus on selecting scaling choices that yield a linear $\rho \sim T$ regime:

[13] For our gravitational solutions the values $\Phi = -2/3$ and $\theta = 0$ are not compatible with each other.
[14] Note that our θ is opposite to that of [22].

JHEP04(2017)009

- Working in the large T approximation (5.2), we have

$$\sigma_2^{\rm DC} \sim T^{\frac{2z-2+\theta}{z}} \left[1 + \frac{Q_2^2}{T^{\frac{2+\theta}{z}} \left(\alpha^2 + Q_1^2 T^{\frac{2z+\theta}{z}} \right)} \right] . \tag{5.11}$$

  Since in the range (5.3) the contribution from the α term in the denominator is always subleading compared to that of Q_1, the leading terms in the expansion of $\sigma_2^{\rm DC}$ are given by

$$\sigma_2^{\rm DC} \sim T^{\frac{2z-2+\theta}{z}} + \frac{Q_2^2}{Q_1^2} T^{\frac{-\theta-4}{z}} + \ldots = T^{\frac{\zeta_2-2}{z}} + \frac{Q_2^2}{Q_1^2} T^{\frac{\zeta_1-2}{z}} + \ldots , \tag{5.12}$$

  and are therefore insensitive to the magnitude α of the axionic sources. When $z = \theta + 4$ a linear regime $\rho \sim T$ arises from the Q_2 dependent term at intermediate temperatures, since the first term dominates the large T behavior (its power is constrained to be positive by the null energy conditions).

- The contribution encoded by α comes into play when we consider subleading terms. As an example, we examine the form of $\sigma_2^{\rm DC}$ in the small α approximation (5.4). Starting from the expression (4.3) and expanding to linear order in α^2, we find

$$\sigma_2^{\rm DC} \sim T^{\frac{2z-2+\theta}{z}} + \frac{Q_2^2}{Q_1^2} T^{\frac{-\theta-4}{z}} + \alpha^2 T^{-\frac{2}{z}} - \frac{\alpha^2 Q_2^2}{Q_1^2} T^{-\frac{2}{z}(2+z+\theta)} \ldots , \tag{5.13}$$

  where we are suppressing positive coefficients that depend on (z, θ). The competition between the different terms in the expansion will then be sensitive to the size of Q_2 and α as well as the particular values of the scaling exponents. When $z = 2$ we see a contribution to the DC conductivity of the form $\alpha^2 T^{-2/z} \sim \alpha^2 T^{-1}$, again compatible with a linear resistivity in an appropriate intermediate temperature regime.

Whether $\sigma_2^{\rm DC}$ can give rise to a linear DC resistivity in other regimes entails a detailed study of the relation (5.1). Inspecting the behavior of $\sigma_2^{\rm DC}$ for generic temperatures, we see that it differs in a crucial way from the result of [24]. The Q_1^2 term in the denominator of our expression (5.11), which is temperature dependent, does not appear in [24], precisely because both gauge fields were not allowed to fluctuate in their analysis. One cannot merely set $Q_1 = 0$ in this expression, without also setting $z = 1$. Furthermore, by naively suppressing the Q_1 term and incorrectly identifying $\sigma_2^{\rm DC}$ with

$$\sigma_{22} \sim T^{\frac{2z-2+\theta}{z}} + \frac{Q_2^2}{\alpha^2} T^{\frac{2z-4}{z}} + \ldots , \tag{5.14}$$

one is in fact turning off a contribution that is more important — in the large temperature regime (5.2) used to arrive at this expression — than that coming from the α term. Moreover, notice that the $z = 1$ and $\theta = -1$ case considered in [24], which naively yields a linear temperature dependence for the resistivity, $\sigma_{22}(z = 1,\ \theta = -1) \sim \frac{1}{T} + \frac{Q_2^2}{\alpha^2} \frac{1}{T^2}$, violates the null energy conditions and is therefore problematic.

JHEP04(2017)009

5.2.1 A numerical example

The cases considered above relied on simple analytical estimates. Here we examine numerically the temperature dependence of $\sigma_2^{\rm DC}$ for specific scaling exponents, using the exact expressions (4.3) and (5.1), to confirm some of the conclusions we reached with our rough temperature approximations. We will choose parameters to obtain a linear regime for the resistivity, as a proof of principle that it can indeed be realized. A more extensive numerical analysis is beyond the scope of this paper.

As a concrete example, we consider the case $z = \frac{4}{3}$ and $\theta = 0$, which is reminiscent of the scalings singled out in [41], and choose the parameters $Q_2 = 1000$ and $\alpha = 10$. For $T \leq T_0 \sim 17.5$, the resistivity can be approximated by a linear function with

$$\rho = 0.0222(1 + 0.283T)\,, \tag{5.15}$$

and at $T = T_0$ it turns around,[15]

$$\frac{\partial \rho}{\partial T}\Big|_{T=T_0} = 0\,. \tag{5.16}$$

For $T > T_0$ we find it convenient to approximate it using the Steinhart-Hart equation [30],

$$\frac{1}{T} = A + B\log(\rho) + C(\log(\rho))^3 + D(\log(\rho))^2\,, \tag{5.17}$$

with coefficients

$$A = 0.818\,, \qquad B = 0.702\,, \qquad C = 0.0202\,, \qquad D = 0.205\,. \tag{5.18}$$

We plot $\rho(T)$ and the two approximate functions in figure 1.

As we can see in figure 2 where the low temperature region is magnified, the linear regime described by the straight line (5.15) appearing in figure 1 matches with the resistivity roughly between $T \in (4.0, 10)$. As smaller temperatures we have instead an expansion of the form $\rho \sim 0.03(1 + 0.1T + 0.01T^2 + 0.00006T^3)$ and the third-order term can be ignored. In the higher-temperature phase the approximation to (5.17) is accurate over a wider range. In this example we have chosen $Q_2 = 1000$ and $\alpha = 10$, with a large ratio $Q_2/\alpha = 100$. If we consider a smaller value $Q_2 = 10$, so that $Q_2/\alpha = 1$ instead, the nearly linear small T region disappears and once finds the decaying behavior seen in figure 3. Note that for the case with $\alpha = 0$, corresponding to an infinite ratio of Q_2/α, we get the ρ temperature dependence shown in figure 1.

We close this section with a few comments on the extremal limit for which $T = 0$. Let us denote the horizon radius by $r_0 = \bar{r}_0$. We have (for $T \sim 0$) that

$$\frac{z + 2 + \theta}{4\pi}\bar{r}_0^z = \frac{Q_2^2}{8\pi(2+\theta)\,\bar{r}_0^{z+2+2\theta}} + \frac{\alpha^2}{4\pi(2+\theta)\,\bar{r}_0^{z+\theta}}\,. \tag{5.19}$$

We can solve for Q_2 in terms of $\bar{r}_0$ and α^2. It is then easy to establish that for small T, we have

$$r_0 = \bar{r}_0 + \frac{4\pi\bar{r}_0^{z+1+\theta}}{[-\alpha^2 + 2(z+1+\theta)(z+2+\theta)\,\bar{r}_0^{2z+\theta}]}\,T\,. \tag{5.20}$$

[15] Similar transitions were seen in massive gravity in [44].

JHEP04(2017)009

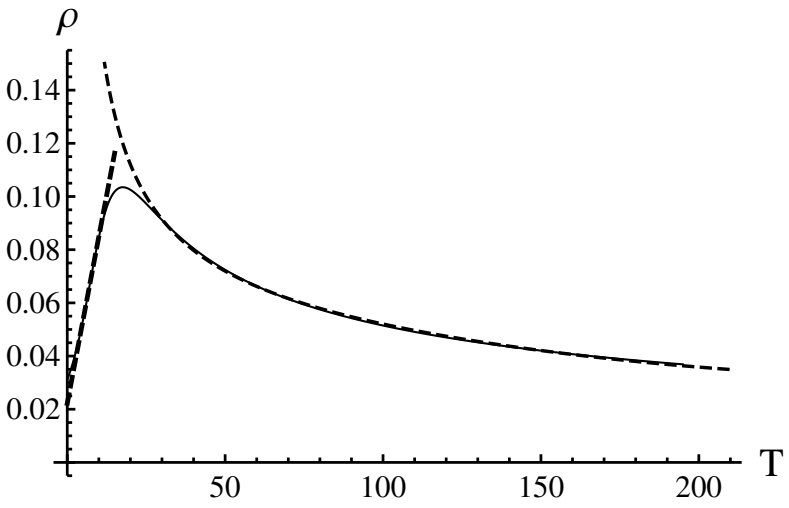

Figure 1. Plot of resistivity versus temperature for $z = 4/3, \theta = 0, Q_2 = 1000$ and $\alpha = 10$, showing a transition from a linear regime to a decaying region. The resistivity $\rho_2(T)$ is plotted as a solid thin line. The straight dashed line on the left represents (5.15), while the curved dashed line on the right represents (5.17).

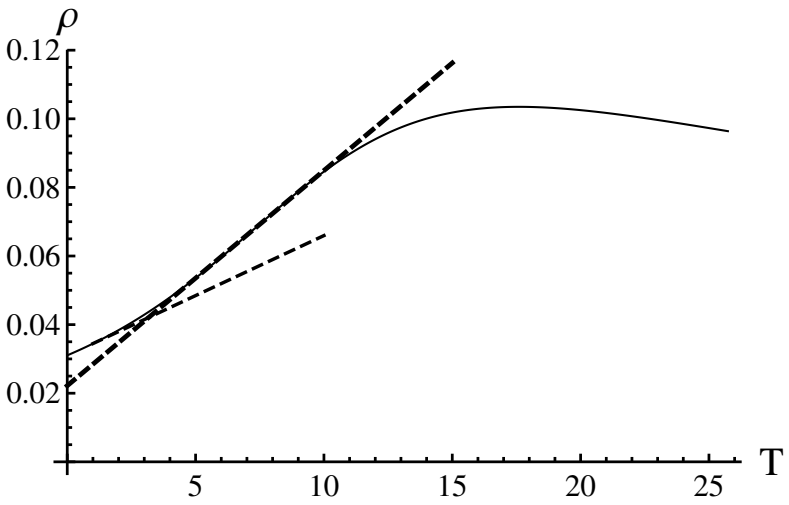

Figure 2. Plot of resistivity versus low temperature for $z = 4/3, \theta = 0, Q_2 = 1000$ and $\alpha = 10$, The longer straight dashed line represents (5.15).

Thus, perhaps not surprisingly, we have

$$\sigma_{ij} \sim \bar{\sigma}_{ij} + \mathcal{O}(T)\,. \tag{5.21}$$

This linear dependence can be seen as the shorter dashed line in figure 2.

While we have seen a number of cases for which one can find $\sigma_{DC} \sim T^{-1}$, it would be useful to have a deeper understanding of which features, if any, are robust to changes in z and θ. Moreover, while the latter exponents control the possible scaling behaviors of the resistivity, the question of the temperature range in which a given scaling is possible

JHEP04(2017)009

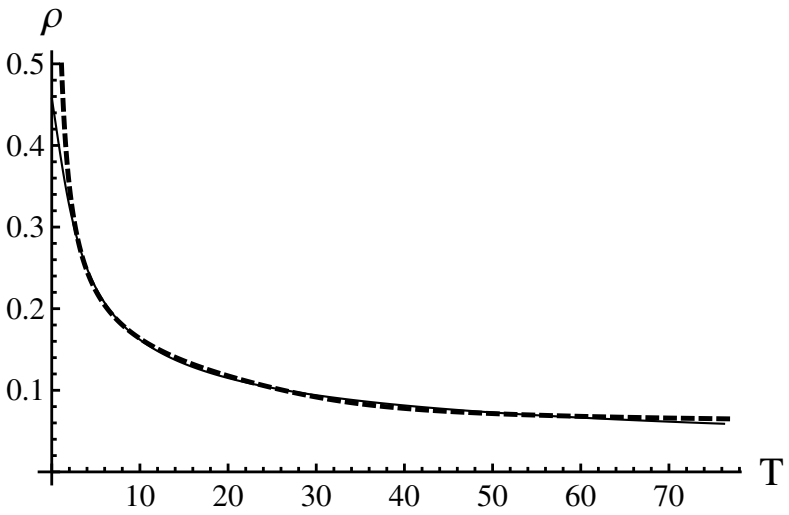

Figure 3. Plot of resistivity versus temperature for $z = 4/3, \theta = 0, Q_2 = 10$ and $\alpha = 10$. For these parameters the linear regime is no longer present. The dashed curved line represents the fit (5.17) with coefficients $A = 2.29, B = 2.67, C = 0.145, D = 1.07$.

is more complicated. In the two-charge case, enough parameters can be tuned that a wide array of scalings are possible, in different temperature regimes. While we have seen that a linear regime is possible, this is far by being able to explain the universality of $\rho \sim T$.

6 Conclusions and summary of results

In an attempt to gain insight into strongly coupled phases with anomalous scalings, we have chosen to work with an holographic model that gives rise to non-relativistic geometries that violate hyperscaling. These provide a fruitful laboratory for realizing geometrically a variety of scalings, and insights into the potential mechanisms behind them. The solutions we have examined are supported by a running dilatonic scalar and two gauge fields, with the latter playing very different roles. One gauge field is responsible for generating the Lifshitz-like nature of the background, with its charge Q_1 entirely fixed in terms of the scaling exponents. The other one plays a role analogous to that of a standard Maxwell field in asymptotically AdS space, and its charge Q_2 is a free parameter. Since our interest here is in the computation of DC conductivities, we have included two spatially dependent axionic fields which encode the physics of momentum dissipation in the dual theory, without spoiling the homogeneity of the background. Consistency of the resulting perturbation equations requires both gauge fields to fluctuate, which leads to some subtleties in the analysis.

As we have seen in section 3, the conductive response of the system is characterized by a matrix σ_{ij} whose components are

$$\sigma_{11} = \frac{1}{r_0^{4+\theta}} + \frac{Q_1^2 r_0^{2z-4}}{\alpha^2}\,, \quad \sigma_{12} = \sigma_{21} = \frac{Q_1 Q_2 r_0^{2z-4}}{\alpha^2}\,, \quad \sigma_{22} = r_0^{2z-2+\theta} + \frac{Q_2^2}{\alpha^2} r_0^{2z-4}\,, \tag{6.1}$$

JHEP04(2017)009

$Q_2 = 0$, AdS asymptotics	
$z = 4 + \theta$, $-4 < \theta < -\frac{8}{3}$	$\rho \sim T$ at large T
$z = \frac{4}{3}$, $\theta > 0$	$\rho \sim T$ at large T
$z = \frac{4}{3}$, $\theta = -\frac{4}{3}$	$\rho \sim T$ at large T and $\rho \sim T^2$ at intermediate T
$z = \frac{4}{3}$, $\theta = -\frac{8}{3}$	$\rho \sim T$ for all T

Table 1. *Single charge case, AdS asymptotics.* A few representative cases (examined in 5.1), which yield a linear regime for the resistivity. These correspond to geometries that exhibit scaling behavior characterized by (z, θ) in the IR, but approach AdS in the UV.

with α the magnitude of the axionic scalars. The temperature dependence is therefore controlled by the interplay between the horizon size r_0 and the three quantities Q_1 (fixed by the background), Q_2 and α. In particular, in the "large temperature" regime $r_0^{2z+\theta} \gg \alpha^2$ and $r_0^{2z+2+2\theta} \gg Q_2^2$ we recover the standard Lifshitz scaling $T \sim r_0^z$, while subleading temperature effects are encoded by (5.4). A detailed study of the temperature dependence can be performed numerically by inverting expression (5.1) once the scaling exponents are specified, as done in 5.2.1, but is not feasible analytically in full generality. Here we have only considered a few special cases, relying mostly on simple estimates.

Since the result (6.1) was obtained from a horizon computation, it is only sensitive to the IR behavior of the geometry. Thus, it also describes systems in which the IR is Lifshitz-like, while the UV is relativistic. The main difference between our explicit setup, in which the solutions are everywhere Lifshitz-like, and the more standard relativistic case with AdS asymptotics comes from examining the boundary behavior of the perturbations. Indeed, the physical interpretation of the components of σ_{ij} is very different depending on the UV symmetries and asymptotic behavior of the geometry, as discussed in section 4.

For example, in the single charge case $Q_2 = 0$ with Lifshitz asymptotics (in which the second gauge field is truncated out from the theory), the current associated with the first gauge field is not an electrical current. Rather, it has the interpretation of an energy flux, and the component σ_{11} does not represent the DC conductivity in the system. However, if the theory is modified slightly, so that the same IR geometries can be embedded in AdS, we recover the standard interpretation, $\sigma^{DC} = \sigma_{11}$. We have examined the temperature dependence in the $Q_2 = 0$ case, under the assumption of AdS asymptotics, in section 5.1, obtaining at large T

$$\sigma^{\rm DC} = \sigma_{11} \sim \frac{Q_1^2}{\alpha^2} T^{\frac{2z-4}{z}} + T^{-\frac{4+\theta}{z}} , \tag{6.2}$$

in agreement with the IR analysis of [22]. Some of the cases in which this expression yields a linear resistivity $\rho \sim T$ are summarized in table 1.

While in this paper we have done a preliminary analysis of the fluctuations at the boundary, contained in appendix B, we haven't taken into account holographic renormalization, which is expected to play an important role. Still, according to our analysis ensuring a well-behaved asymptotic expansion in the non-relativistic case requires taking the current associated with the Lifshitz gauge field to vanish, $j_1 = 0$, when the dynamical

JHEP04(2017)009

$j_1 = 0$, Lifshitz asymptotics	
$z = 4 + \theta$	$\rho \sim T$ at intermediate T from Q_2 dependent terms
$z = 2$, α small	$\rho \sim T$ at intermediate T from α dependent terms
$z = \frac{4}{3}$, $\theta = 0$ and $\frac{Q_2}{\alpha}$ large	$\rho \sim T$ for small T

Table 2. *Lifshitz asymptotics, linearly dependent sources.* A few representative cases (examined in 5.2) which yield a linear regime for the resistivity. These correspond to geometries that are asymptotically Lifshitz and hyperscaling violating.

critical exponent is in the range $1 \leq z \leq 4/3$. The condition $j_1 = 0$ implies that the two sources E_1 and E_2 can not be turned on independently, a feature that is absent in AdS and which we would like to understand better. In particular, it could very well be an artifact of not having performed holographic renormalization.

In section 4 we have analyzed in some detail the behavior of σ_{ij} when $j_1 = 0$ (with the sources constrained through $\sigma_{11}E_1 + \sigma_{12}E_2 = 0$), for solutions with Lifshitz asymptotics. The DC conductivity in the temperature regime $T \sim r_0^z$ is then given by

$$\sigma_2^{\rm DC} \sim T^{\frac{2z-2+\theta}{z}} \left[1 + \frac{Q_2^2}{T^{\frac{2+\theta}{z}} \left(\alpha^2 + Q_1^2 T^{\frac{2z+\theta}{z}}\right)}\right] , \tag{6.3}$$

and is controlled by the interplay between the two charges and the size of the axionic fields. Again, we summarize some of the cases corresponding to linear resistivities in table 2.

Even though the physical interpretation of the matrix (6.1) in full generality is not yet clear for Lifshitz asymptotics (and some of these issues will be addressed in [36]), what is apparent from our analysis is that the temperature behavior is quite rich, and moreover that a linear temperature dependence for the resistivity is not difficult to find, as exemplified by tables 1 and 2. An important point to keep in mind is that the range of temperatures for which results like (6.3) apply can be tuned by adjusting the two parameters α and Q_2 as desired. Indeed, "large" temperatures are only large compared to appropriate powers of α and Q_2, and therefore one can push the linear resistivity regime to smaller or larger temperatures by simply changing the size of these two tunable parameters. The existence of the additional scale set by Q_2 is one of the advantages of working with a model that involves two gauge fields. An additional feature to note is that since our $\{z, \theta\}$ scaling solutions occupy the entire geometry and not just its IR portion, they can in principle describe intermediate scalings (much as in [43], where the focus however was on the behavior of the optical conductivity).

We emphasize once again here, as we did in section 4, that by neglecting the fluctuations of both gauge fields one obtains an incorrect result for $\sigma_2^{\rm DC}$, which ignores an important temperature dependent term controlled by Q_1. We leave a more detailed analysis of the temperature dependence of the DC conductivities and a study of the thermal conductivity (along the lines of [27, 45]) to future work. Another question is whether there

JHEP04(2017)009

are any mechanisms in our model analogous to those of [46], who also examined transport in a gravitational theory with two bulk gauge fields and a dilatonic scalar. One of the interesting features of the construction of [46] is the presence of a finite conductivity — specifically, the DC *transconductance* — without the need to break translational invariance.

Perhaps the most important point to stress is that a more general understanding of the transport properties in theories such as ours must take into account extensions of the holographic dictionary to non-relativistic spacetimes (see e.g. [47, 48] in the presence of hyperscaling violation). Insights from non-relativistic hydrodynamics might help us understand the role of momentum dissipation in determining the final form of $\sigma^{\rm DC}$. For instance, an analysis along the lines of [49] may shed light on the relation between horizon and boundary data, and on the interpretation of the latter in our model.

Before closing we should mention that another interesting question in these holographic models is that of the scaling of the Hall angle, as compared to that of the DC conductivity. Although here we have not included a magnetic field, by inspecting the structure of the matrix σ_{ij} in (3.13) we expect a behavior similar to that observed in [39], due to the presence of two scales in our system. In particular, in analogy with what was seen in [39] in a different context, σ_{12} scales just like the α-dependent parts of σ_{11} and σ_{22}. Finally, we find it intriguing that in many cases the special choice $z = 4/3$ discussed by [41] also leads to a linear resistivity in our model. Perhaps more interestingly, in our construction $z = 4/3$ is the edge of the range seemingly associated with perturbations that diverge at the non-relativistic boundary. While the special role played by $z = 4/3$ may just be a coincidence — and the boundary analysis is only preliminary — it deserves further attention, as it is of interest to find explicit gravitational realizations of the scalings singled out in [41], and gain insight into their origin. We leave these questions to future work.

Acknowledgments

We are grateful to Mike Blake, Mirjam Cvetic, Richard Davison, Aristos Donos, Jerome Gauntlett and Sean Hartnoll for comments on the draft and useful conversations. We especially thank Blaise Gouteraux and Ioannis Papadimitriou for extensive discussions. S.C. would like to thank Cambridge University and the Tokyo Institute of Technology for hospitality during the final stages of this work. The work of S.C. is supported in part by the National Science Foundation grant PHY-1620169. H-S.L. is supported in part by NSFC grants No. 11305140, 11375153, 11475148, 11675144 and CSC scholarship No. 201408330017. The work of H.L. is supported in part by NSFC grants NO. 11175269, NO. 11475024 and NO. 11235003. C.N.P. is supported in part by DOE grant DE-FG02-13ER42020.

A A general class of hyperscaling-violating solutions

In this appendix, we present a class of electrically-charged Lifshitz-Like black branes with hyperscaling violations, carrying magnetic p-form fluxes along the brane space. The Lagrangian consists of the metric, a dilaton, two Maxwell fields and N p-form field strengths.

JHEP04(2017)009

The Lagrangian in general n dimensions is given by

$$\mathcal{L} = \sqrt{g}\Big(R - \frac{1}{2}(\partial\phi)^2 - 2\Lambda e^{\lambda_0\phi} - \frac{1}{4}e^{\lambda_1\phi}F_{1(2)}^2 - \frac{1}{4}e^{\lambda_2\phi}F_{2(2)}^2 - \sum_{i=1}^{N}\frac{e^{\lambda_3\phi}}{2p!}\mathcal{F}_{i\,(p)}^2\Big)\,. \tag{A.1}$$

We consider the ansatz

$$\begin{aligned} ds^2 &= r^{2\theta}\big(-r^{2z}\,f\,dt^2 + \frac{dr^2}{r^2\,f} + r^2 dx_i dx_i\big)\,,\\ \phi &= \gamma\log r\,, \qquad A_1 = \Phi_1 dt\,, \qquad A_2 = \Phi_2 dt\,,\\ \mathcal{F}^i_{(p)} &= \alpha\, dx^{(i)}_{j_1}\wedge\ldots\wedge dx^{(i)}_{j_p}\,, \end{aligned} \tag{A.2}$$

where $x^{(i)}_j$, $1\le j\le p$, denote disjoint sets of transverse-space coordinates spanning the total $(n-2)$-dimensional transverse space, and so we shall have

$$Np = n-2\,. \tag{A.3}$$

The equation of motion for the electric field gives

$$\Phi_1' = Q_1\, r^{z+1-n-\lambda_1\gamma-(n-4)\theta}\,, \qquad \Phi_2' = Q_2\, r^{z+1-n-\lambda_2\gamma-(n-4)\theta}\,. \tag{A.4}$$

The solution is

$$\begin{aligned} f = 1 &+ \frac{\alpha^2 r^{-2(\theta p+p+z-1)}}{2p(\theta+1)(2\theta-(n-2p)(\theta+1)+z)}\\ &+\frac{Q_2^2\, r^{-2(-2\theta+\theta n+n+z-3)}}{2(\theta+1)(n-2)((n-2)(\theta+1)+z-2)} - m r^{2\theta-(\theta+1)n-z+2}\,, \end{aligned} \tag{A.5}$$

with parameters satisfying the relations

$$\begin{aligned} \gamma &= \sqrt{2(\theta+1)(n-2)(\theta+z-1)}\,, & \lambda_0 &= -\frac{\sqrt{2}\theta}{\sqrt{(\theta+1)(n-2)(\theta+z-1)}}\,,\\ \lambda_1 &= -\frac{\sqrt{2}((n-3)\theta+n-2)}{\sqrt{(\theta+1)(n-2)(\theta+z-1)}}\,, & \lambda_2 &= -\lambda_3 = \sqrt{\frac{2(\theta+z-1)}{(\theta+1)(n-2)}}\,,\\ Q_1 &= \sqrt{2(z-1)((n-2)(\theta+1)+z)}\,, & & \\ \Lambda &= -\frac{1}{2}((n-2)(\theta+1)+z-1)((n-2)(\theta+1)+z)\,. & & \end{aligned} \tag{A.6}$$

B Asymptotic analysis

This appendix gives a self-contained discussion of some of the asymptotic properties of the solutions, including an explicit demonstration of the way in which the DC ansatz of section 3 emerges as an $\omega\to 0$ limit of a small-ω AC calculation. The presence of multiple gauge fields in our model substantially complicates the analysis. We will highlight some

JHEP04(2017)009

of the subtleties which arise from allowing each gauge field to fluctuate, and comment on how this method relates to the one of section 3. However, we have not taken into account holographic renormalization, which is expected to play an important role in clarifying the interpretation of our results, given Lifshitz asymptotics. A more thorough discussion will appear in [36]. The reader should also be aware that the perturbations in this section are not the same as those of the horizon analysis done there. In particular, to avoid confusion we will use hatted quantities to refer to the perturbations of section 3.

In contrast to the analysis of section 3 — in which the electric fields were taken to be constant — we will now allow the fluctuations of all the fields to have monochromatic time dependence $e^{-\mathrm{i}\omega t}$. To this end, we consider the following perturbations:

$$(\delta A_i)_{x_1} = a_i(r)e^{-\mathrm{i}\omega t}\,, \qquad \delta\chi_1 = b(r)e^{-\mathrm{i}\omega t}\,, \qquad \delta g_{tx} = r^{\theta+2}\,\psi(r)e^{-\mathrm{i}\omega t}\,, \tag{B.1}$$

where it is to be understood that the physical perturbations are given by taking the real parts of these expressions. At the linear level, the equations of motion then imply

$$\begin{aligned}
&(r^{z-3-\theta}fa_1')' + \frac{\omega^2 a_1}{r^{z+5+\theta}f} + Q_1\psi' = 0\,,\\
&(r^{3z-1+\theta}fa_2')' + \frac{\omega^2 a_2}{r^{3-z-\theta}f} + Q_2\psi' = 0\,,\\
&\psi' = -\frac{1}{r^{5-z+\theta}}\left(Q_1a_1 + Q_2a_2 - \frac{r^{5-z}\alpha f b'}{\mathrm{i}\omega}\right)\,,\\
&\psi = -\frac{\mathrm{i}\omega\, b}{\alpha} + \frac{f\,(r^{5-z}fb')'}{\mathrm{i}\omega\,\alpha r^{3(1-z)}}\,.
\end{aligned} \tag{B.2}$$

We can eliminate ψ, and obtain

$$\begin{aligned}
(r^{z-3-\theta}fa_1')' + \frac{\omega^2}{r^{z+5+\theta}f}a_1 &= \frac{Q_1}{r^{5-z+\theta}}\left(Q_1a_1 + Q_2a_2 - \alpha\tilde{b}\right)\,,\\
(r^{3z-1+\theta}fa_2')' + \frac{\omega^2}{r^{3-z-\theta}f}a_2 &= \frac{Q_2}{r^{5-z+\theta}}\left(Q_1a_1 + Q_2a_2 - \alpha\tilde{b}\right)\,,\\
\left(r^{3(z-1)}f\tilde{b}'\right)' + \frac{\omega^2}{r^{5-z}f}\tilde{b} &= -\frac{\alpha}{r^{5-z+\theta}}\left(Q_1a_1 + Q_2a_2 - \alpha\tilde{b}\right)\,,
\end{aligned} \tag{B.3}$$

where $\tilde{b} = r^{5-z}fb'/(\mathrm{i}\omega)$. Note that one can again see from (B.3) that, as remarked previously, it would be inconsistent to set the perturbation a_1 to zero, since it would imply $\tilde{b} = Q_2\,a_2/\alpha$, and hence the last two equations in (B.3) would be incompatible.

For later purposes, it is useful, as in [20], to introduce the two independent quantities

$$\begin{aligned}
\Pi_1 &= -r^{z-3-\theta}fa_1' - \frac{Q_1}{\alpha}r^{3(z-1)}f\tilde{b}'\,,\\
\Pi_2 &= -r^{3z-1+\theta}fa_2' - \frac{Q_2}{\alpha}r^{3(z-1)}f\tilde{b}'\,,
\end{aligned} \tag{B.4}$$

which are radially conserved up to (and including) $\mathcal{O}(i\omega)$.[16] In other words, we must have

$$\Pi_i = \mathrm{i}\omega\, j_i + \mathcal{O}(\omega^2)\,, \qquad i = 1, 2. \tag{B.5}$$

[16] Note that the functions Π_i are essentially the same as the currents $\langle J_i\rangle$ in the Kubo formula (3.1), since they arise as the surface terms in the variation of the quadratic action for the fluctuations with respect to the external sources.

JHEP04(2017)009

where j_i are constants. In fact, they are the same as the conserved currents j_i introduced in (3.4). These two conserved quantities are associated with the two zero-eigenvalue modes of the mass matrix for the perturbations, which can be read off from (B.3).

Next, we define the two quantities

$$H_1(\omega) = \lim_{r\to\infty} \frac{r^{z-3-\theta} a_1'}{a_1}\,, \qquad H_2(\omega) = \lim_{r\to\infty} \frac{r^{3z-1+\theta} a_2'}{a_2}\,, \tag{B.6}$$

which we associate with the following large-r asymptotic behavior for a_i:

$$\begin{aligned} a_1 &= a_{10}\Big(1 + \frac{H_1(\omega)}{(z-4-\theta) r^{z-4-\theta}} + \cdots\Big)\,,\\ a_2 &= a_{20}\Big(1 + \frac{H_2(\omega)}{(3z-2+\theta) r^{3z-2+\theta}} + \cdots\Big)\,. \end{aligned} \tag{B.7}$$

Notice that in order for a_1 to be regular asymptotically, one must have $H_1(\omega) = 0$ when $z - 4 - \theta < 0$. On the other hand, the regularity of a_2 is guaranteed by the null energy condition and having taken $z \geq 1$. We will return to the vanishing of H_1 in more detail shortly. In the $\omega \to 0$ limit, we can then define

$$\gamma_i = -\lim_{\omega\to 0} \frac{H_i(\omega)}{\mathrm{i}\omega}\,, \qquad i = 1, 2. \tag{B.8}$$

The quantities γ_i are the asymptotic data, and later, we shall examine their relation to the conductivity matrix σ_{ij}.

Next, let us consider the ansatz for perturbations that are purely ingoing on the horizon, valid for small ω:

$$\begin{aligned} a_1 &= \frac{E_1}{\mathrm{i}\omega}\, e^{-\frac{\mathrm{i}\omega}{4\pi T}\log f}\big(1 + \mathrm{i}\omega U_1(r) + \mathcal{O}(\omega^2)\big)\,,\\ a_2 &= \frac{E_2}{\mathrm{i}\omega}\, e^{-\frac{\mathrm{i}\omega}{4\pi T}\log f}\big(1 + \mathrm{i}\omega U_2(r) + \mathcal{O}(\omega^2)\big)\,,\\ \tilde{b} &= \frac{\nu}{\mathrm{i}\omega}\, e^{-\frac{\mathrm{i}\omega}{4\pi T}\log f}\big(1 + \mathrm{i}\omega V(r) + \mathcal{O}(\omega^2)\big)\,, \end{aligned} \tag{B.9}$$

where the Hawking temperature T is given by (2.9). We require (E_1, E_2, ν) to be real constants, and the U_i to be real functions that are regular both on the horizon and at asymptotic infinity. Note that the $\mathrm{i}\omega$ denominators on the right-hand sides of eqns (B.9) are included for convenience, in order to facilitate the comparison with the DC ansatz approach that we described in section 3. In particular, the constants E_1 and E_2 in (B.9) will turn out to be the same, in the $\omega \to 0$ limit, as the constants we introduced in the DC ansatz in (3.3). To see this, we recall that the physical fluctuations of the various fields are obtained from the complex expressions (B.1) and (B.9) by taking the real parts of the right-hand sides in (B.1). Thus, for example, the physical fluctuations $(\delta A_i)_x$ are given by

$$\begin{aligned} (\delta A_i)_x &= \Re\left[\frac{E_i}{\mathrm{i}\omega}\left(1 - \frac{\mathrm{i}\omega\log f}{4\pi T} + \mathrm{i}\omega U_i - \mathrm{i}\omega t + \mathcal{O}(\omega^2)\right)\right]\,,\\ &= -E_i t - E_i\left(\frac{\log f}{4\pi T} - U_i\right) + \mathcal{O}(\omega)\,. \end{aligned} \tag{B.10}$$

JHEP04(2017)009

Taking the DC limit $\omega \to 0$, we reproduce the expressions for $(\delta A_i)_x$ given in (3.3), with

$$\hat{a}_i = -E_i \left(\frac{\log f}{4\pi T} - U_i \right) , \tag{B.11}$$

and we are using hatted quantities to refer to the perturbations of section 3. In an analogous manner we can confirm that, as mentioned earlier, the constants j_i appearing in (3.4) are indeed the same as the ones arising in (B.5).

Returning to the complex expressions (B.9), we now substitute these into the perturbation equations (B.3). At the leading order in ω, i.e. at order ω^{-1}, we find

$$E_1 Q_1 + E_2 Q_2 - \nu\alpha = 0 . \tag{B.12}$$

At the next order, i.e. ω^0, we have

$$\begin{aligned}
&\left(E_1 r^{z-3-\theta} f U_1'\right)' - \frac{Q_1}{r^{5-z+\theta}} \left(E_1 Q_1 U_1 + E_2 Q_2 U_2 - \nu\alpha V\right) - \left(\frac{E_1 r^{z-3-\theta} f'}{4\pi T}\right)' = 0 , \\
&\left(E_2 r^{3z-1+\theta} f U_2'\right)' - \frac{Q_2}{r^{5-z-\theta}} \left(E_1 Q_1 U_1 + E_2 Q_2 U_2 - \nu\alpha V\right) - \left(\frac{E_2 r^{3z-1+\theta} f'}{4\pi T}\right)' = 0 , \\
&\left(\nu r^{3(z-1)} f V'\right)' + \frac{\alpha}{r^{5-z+\theta}} \left(E_1 Q_1 U_1 + E_2 Q_2 U_2 - \nu\alpha V\right) + \left(\frac{\nu r^{3(z-1)} f'}{4\pi T}\right)' = 0 .
\end{aligned} \tag{B.13}$$

It follows from (B.5) that the first two integrals are

$$\begin{aligned}
&\frac{r^{z-3-\theta}}{\alpha} \left(\left(E_1 \alpha U_1' + \nu Q_1 r^{2z+\theta} V'\right) f - \frac{\left(E_1 \alpha + \nu Q_1 r^{2z+\theta}\right) f'}{4\pi T} \right) = -j_1 , \\
&\frac{r^{3(z-1)}}{\alpha} \left(\left(E_2 \alpha r^{2+\theta} U_2' + \nu Q_2 V'\right) f - \frac{(E_2 \alpha r^{2+\theta} + \nu Q_2) f'}{4\pi T} \right) = -j_2 .
\end{aligned} \tag{B.14}$$

Evaluating the above equations on the horizon, we find

$$j_1 = \frac{\alpha E_1 + \nu\, Q_1\, r_0^{2z+\theta}}{\alpha r_0^{4+\theta}} , \qquad j_2 = \frac{1}{\alpha} (\nu\, Q_2 + \alpha\, E_2\, r_0^{2+\theta})\, r_0^{2z-4} . \tag{B.15}$$

Using (B.12) to substitute for ν in these equations, we obtain expressions for the j_i in terms of the E_i which are precisely those given by eqns (3.12) and (3.13).

The calculation above shows how the conductivities are read off from the horizon data. We next turn to a discussion of how they are related to data on the boundary at infinity. In particular, we shall see that regularity requirements at the boundary can provide additional constraints on the currents j_1 and j_2, and hence modify the conductivity matrix.

To calculate the quantities γ_i defined in (B.8) and (B.6), we first take the $\omega = 0$ limit, and define the functions W_1 and W_2 by

$$\begin{aligned}
\lim_{\omega\to 0} \frac{r^{z-3-\theta} a_1'}{(-\mathrm{i}\omega\, a_1)} &= r^{z-3-\theta} \Big(\frac{f'}{4\pi T\, f} - U_1' \Big) \equiv r^{2(z-1)} W_1 , \\
\lim_{\omega\to 0} \frac{r^{3z-1+\theta} a_2'}{(-\mathrm{i}\omega\, a_2)} &= r^{3z-1+\theta} \Big(\frac{f'}{4\pi T\, f} - U_2' \Big) \equiv r^{2(z-1)} W_2 .
\end{aligned} \tag{B.16}$$

JHEP04(2017)009

It turns out that W_1 and W_2 satisfy

$$
\begin{aligned}
(r^{3z+1+\theta} f^2\, W_1')' &= \frac{j_1\,(Q_2^2+\alpha^2\, r^{2+\theta}) - j_2\, Q_1\, Q_2}{E_1\, r^{z+1+2\theta}}\,,\\
(r^{3z+1+\theta} f^2\, W_2')' &= -\frac{j_2\,\alpha^2 + Q_1\,(j_2\, Q_1 - j_1\, Q_2)\, r^{2z+\theta}}{E_2\, r^{z-1}}\,,
\end{aligned}
\tag{B.17}
$$

which in turn imply that

$$
\begin{aligned}
r^{3z+1+\theta} f^2\, W_1' &= d_1 - \frac{1}{E_1\, r^{z+\theta}}\left(\frac{Q_2\;(j_1\, Q_2 - j_2\, Q_1)}{z+\theta} + \frac{\alpha^2\, j_1\, r^{2+\theta}}{z-2}\right) \equiv \xi_1\,,\\
r^{3z+1+\theta} f^2\, W_2' &= d_2 - \frac{r^2}{E_2}\left(\frac{Q_1\;(j_2\, Q_1 - j_1\, Q_2)\;r^{z+\theta}}{z+2+\theta} - \frac{\alpha^2\, j_2}{(z-2)\;r^z}\right) \equiv \xi_2\,,
\end{aligned}
\tag{B.18}
$$

where d_1 and d_2 are integration constants. Together with (B.16), we have

$$
\begin{aligned}
\left(\frac{U_1'}{r^{z+1+\theta}}\right)' &= \tilde{\zeta}_1 \equiv \left(\frac{f'}{4\pi T\, r^{z+1+\theta} f}\right)' - \frac{\xi_1}{r^{3z+1+\theta} f^2}\,,\\
\left(r^{z+1+\theta} U_2'\right)' &= \tilde{\zeta}_2 \equiv \left(\frac{r^{z+1+\theta} f'}{4\pi T\, f}\right)' - \frac{\xi_2}{r^{3z+1+\theta} f^2}\,.
\end{aligned}
\tag{B.19}
$$

It turns out that by choosing the integration constants appropriately, the singularity at $r = r_0$ in the function $\tilde{\zeta}_i$ can be avoided. This ensures that U_1 and U_2 are regular on the horizon. The leading-order large-r expansions for $\tilde{\zeta}_1$ and $\tilde{\zeta}_2$ depend upon the interval in which the Lifshitz exponent z lies. We find

$$
\tilde{\zeta}_1 = \begin{cases} -\frac{j_1 \alpha^2}{(z-2)E_1}\left(\frac{1}{r}\right)^{4z-1+\theta} + \cdots\,, & 1 \le z < 2;\\ -\frac{d_1}{r^{3z+1+\theta}} + \cdots\,, & 2 < z \le 4;\\ \frac{\text{const.}}{r^{2z+5+\theta}} + \cdots\,, & z > 4; \end{cases}
\tag{B.20}
$$

$$
\tilde{\zeta}_2 = \begin{cases} -\frac{2(z-1)(E_1 Q_2 - E_2 Q_1 r_0^{2z+2+2\theta})}{E_2 Q_1 r_0^{4+\theta}} \frac{1}{r^{2z-1}} + \cdots\,, & z < 2\\ \frac{\text{const.}}{r^3} + \cdots\,, & z > 2 \end{cases}
\tag{B.21}
$$

which imply that for $z > 1$ and $\theta > 0$, $\tilde{\zeta}_i$ can be integrated out to infinity without divergence. Thus the general solutions for U_i' are given by

$$
U_1' = r^{z+1+\theta}\left(\beta_1 + \int_\infty^r \tilde{\zeta}_1\right)\,, \qquad U_2' = \frac{1}{r^{z+1+\theta}}\left(\beta_2 + \int_\infty^r \tilde{\zeta}_2\right)\,,
\tag{B.22}
$$

where the β_i's are two integration constants. It is clear that the regularity of U_1 at asymptotic infinity requires that $\beta_1 = 0$.

We are now in a position to obtain the two quantities

$$
\begin{aligned}
\gamma_1 &= \lim_{\substack{r\to\infty\\ \omega\to 0}} \frac{r^{z-3-\theta} a_1'}{(-\mathrm{i}\omega\, a_1)} = 0\,,\\
\gamma_2 &= \lim_{\substack{r\to\infty\\ \omega\to 0}} \frac{r^{3z-1+\theta} a_2'}{(-\mathrm{i}\omega\, a_2)} = \frac{j_2\, Q_1 - j_1\, Q_2}{E_2 Q_1} = r_0^{(2z-2+\theta)}\left(1 - \frac{E_1 Q_2}{E_2 Q_1}\frac{1}{r_0^{2(z+1+\theta)}}\right)\,,
\end{aligned}
\tag{B.23}
$$

JHEP04(2017)009

working under the assumption that $z > \frac{4}{3}$. Indeed, for $1 \leq z \leq \frac{4}{3}$, we find that the the leading falloff of U_1 becomes divergent. Specifically, for $1 \leq z < \frac{4}{3}$ we find

$$U_1 = -\frac{\alpha^2 j_1}{(z-2)(4z-2+\theta)(3z-4)} r^{4-3z} + \cdots , \tag{B.24}$$

whilst for $z = \frac{4}{3}$ we find

$$U_1 = -\frac{9\alpha^2\, j_1}{2(10+3\theta)} \log r + \cdots . \tag{B.25}$$

The convergence of U_1 at large r for $1 \leq z \leq \frac{4}{3}$ requires either $\alpha = 0$ or $j_1 = 0$ (we should mention, however, that properly taking into account holographic renormalization may change this naive picture). Since we are interested in the effect of a nonzero α, for now we consider $j_1 = 0$. It follows from (B.15) that

$$\gamma_2 = r_0^{2z-2+\theta} \left(1 + \frac{Q_2^2}{r_0^{2+\theta}(\alpha^2 + Q_1^2\, r_0^{2z+\theta})}\right) , \qquad 1 \leq z \leq \frac{4}{3} . \tag{B.26}$$

Note that in the AdS limit where $z = 1$ and $\theta = 0$, and hence $Q_1 = 0$, we successfully reproduce the previous known result in the literature.

On the other hand if we have $\alpha = 0$, then we can have all $z \geq 1$, including $z = 2$. It follows from (B.12) and (B.23) that

$$\gamma_2 = r_0^{2z-2+\theta} \left(1 - \frac{Q_2^2}{Q_1^2\, r_0^{2z+2+\theta}}\right) . \tag{B.27}$$

This result is applicable for all $z \geq 1$. It coincides with (B.26) when $1 \leq z \leq 4/3$.

It is interesting to examine how the two asymptotically-defined quantities γ_i and ψ_∞ are related to the currents j_i. It follows from (B.6), (B.8) and (B.16) that

$$\gamma_1 = \lim_{r\to\infty} r^{z-3-\theta} \left(\frac{f'}{4\pi T\, f} - U_1'\right) , \qquad \gamma_2 = \lim_{r\to\infty} r^{3z-1+\theta} \left(\frac{f'}{4\pi T\, f} - U_2'\right) . \tag{B.28}$$

We can then use (B.11) to obtain

$$\gamma_1 = -\lim_{r\to\infty} r^{z-3-\theta} \frac{\hat{a}_1'}{E_1} , \qquad \gamma_2 = -\lim_{r\to\infty} r^{3z-1+\theta} \frac{\hat{a}_2'}{E_2} . \tag{B.29}$$

It now follows from (3.4) that

$$\gamma_1 = \lim_{r\to\infty} \frac{j_1 + Q_1\, \hat{\psi}(r)}{E_1 f(r)} , \qquad \gamma_2 = \lim_{r\to\infty} \frac{j_2 + Q_2\, \hat{\psi}(r)}{E_2 f(r)} . \tag{B.30}$$

Since $f(\infty) = 1$, we find the following relation between the boundary quantities γ_i and the conserved currents j_1 and j_2:

$$\gamma_1 = \frac{j_1}{E_1} + \frac{Q_1\, \hat{\psi}_\infty}{E_1} , \qquad \gamma_2 = \frac{j_2}{E_2} + \frac{Q_2\, \hat{\psi}_\infty}{E_2} . \tag{B.31}$$

Recalling that $\hat{\psi}_\infty = -\frac{j_1}{Q_1}$, it is now clear that $\gamma_1 = 0$, regardless of whether $j_1 = 0$ or not. Moreover, when $j_1 = 0$ we recover the result $\gamma_2 = j_2/E_2$, from which we can immediately conclude that in this case γ_2 is precisely the one we found in eqn (4.3).

JHEP04(2017)009

References

[1] S.A. Hartnoll, *Lectures on holographic methods for condensed matter physics*, *Class. Quant. Grav.* **26** (2009) 224002 [arXiv:0903.3246] [INSPIRE].

[2] S. Sachdev, *What can gauge-gravity duality teach us about condensed matter physics?*, *Ann. Rev. Condensed Matter Phys.* **3** (2012) 9 [arXiv:1108.1197] [INSPIRE].

[3] J. McGreevy, *TASI lectures on quantum matter (with a view toward holographic duality)*, arXiv:1606.08953 [INSPIRE].

[4] A. Karch and A. O'Bannon, *Metallic AdS/CFT*, *JHEP* **09** (2007) 024 [arXiv:0705.3870] [INSPIRE].

[5] S.A. Hartnoll, J. Polchinski, E. Silverstein and D. Tong, *Towards strange metallic holography*, *JHEP* **04** (2010) 120 [arXiv:0912.1061] [INSPIRE].

[6] T. Faulkner, N. Iqbal, H. Liu, J. McGreevy and D. Vegh, *Strange metal transport realized by gauge/gravity duality*, *Science* **329** (2010) 1043 [INSPIRE].

[7] T. Faulkner, N. Iqbal, H. Liu, J. McGreevy and D. Vegh, *Charge transport by holographic Fermi surfaces*, *Phys. Rev.* **D 88** (2013) 045016 [arXiv:1306.6396] [INSPIRE].

[8] S.A. Hartnoll and D.M. Hofman, *Locally Critical Resistivities from Umklapp Scattering*, *Phys. Rev. Lett.* **108** (2012) 241601 [arXiv:1201.3917] [INSPIRE].

[9] G.T. Horowitz, J.E. Santos and D. Tong, *Optical Conductivity with Holographic Lattices*, *JHEP* **07** (2012) 168 [arXiv:1204.0519] [INSPIRE].

[10] G.T. Horowitz, J.E. Santos and D. Tong, *Further Evidence for Lattice-Induced Scaling*, *JHEP* **11** (2012) 102 [arXiv:1209.1098] [INSPIRE].

[11] G.T. Horowitz and J.E. Santos, *General Relativity and the Cuprates*, *JHEP* **06** (2013) 087 [arXiv:1302.6586] [INSPIRE].

[12] P. Chesler, A. Lucas and S. Sachdev, *Conformal field theories in a periodic potential: results from holography and field theory*, *Phys. Rev.* **D 89** (2014) 026005 [arXiv:1308.0329] [INSPIRE].

[13] Y. Ling, C. Niu, J.-P. Wu and Z.-Y. Xian, *Holographic Lattice in Einstein-Maxwell-Dilaton Gravity*, *JHEP* **11** (2013) 006 [arXiv:1309.4580] [INSPIRE].

[14] A. Donos and J.P. Gauntlett, *The thermoelectric properties of inhomogeneous holographic lattices*, *JHEP* **01** (2015) 035 [arXiv:1409.6875] [INSPIRE].

[15] A. Donos and S.A. Hartnoll, *Interaction-driven localization in holography*, *Nature Phys.* **9** (2013) 649 [arXiv:1212.2998] [INSPIRE].

[16] A. Donos and J.P. Gauntlett, *Holographic Q-lattices*, *JHEP* **04** (2014) 040 [arXiv:1311.3292] [INSPIRE].

[17] T. Andrade and B. Withers, *A simple holographic model of momentum relaxation*, *JHEP* **05** (2014) 101 [arXiv:1311.5157] [INSPIRE].

[18] D. Vegh, *Holography without translational symmetry*, arXiv:1301.0537 [INSPIRE].

JHEP04(2017)009

[19] R.A. Davison, *Momentum relaxation in holographic massive gravity*, *Phys. Rev.* **D 88** (2013) 086003 [arXiv:1306.5792] [INSPIRE].

[20] M. Blake and D. Tong, *Universal Resistivity from Holographic Massive Gravity*, *Phys. Rev.* **D 88** (2013) 106004 [arXiv:1308.4970] [INSPIRE].

[21] T. Andrade, *A simple model of momentum relaxation in Lifshitz holography*, arXiv:1602.00556 [INSPIRE].

[22] B. Goutéraux, *Charge transport in holography with momentum dissipation*, *JHEP* **04** (2014) 181 [arXiv:1401.5436] [INSPIRE].

[23] A. Amoretti, M. Baggioli, N. Magnoli and D. Musso, *Chasing the cuprates with dilatonic dyons*, *JHEP* **06** (2016) 113 [arXiv:1603.03029] [INSPIRE].

[24] X.-H. Ge, Y. Tian, S.-Y. Wu, S.-F. Wu and S.-F. Wu, *Linear and quadratic in temperature resistivity from holography*, *JHEP* **11** (2016) 128 [arXiv:1606.07905] [INSPIRE].

[25] A. Donos and J.P. Gauntlett, *Novel metals and insulators from holography*, *JHEP* **06** (2014) 007 [arXiv:1401.5077] [INSPIRE].

[26] A. Donos and J.P. Gauntlett, *Navier-Stokes Equations on Black Hole Horizons and DC Thermoelectric Conductivity*, *Phys. Rev.* **D 92** (2015) 121901 [arXiv:1506.01360] [INSPIRE].

[27] E. Banks, A. Donos and J.P. Gauntlett, *Thermoelectric DC conductivities and Stokes flows on black hole horizons*, *JHEP* **10** (2015) 103 [arXiv:1507.00234] [INSPIRE].

[28] A. Donos, J.P. Gauntlett, T. Griffin and L. Melgar, *DC Conductivity of Magnetised Holographic Matter*, *JHEP* **01** (2016) 113 [arXiv:1511.00713] [INSPIRE].

[29] A. Lucas and S. Sachdev, *Conductivity of weakly disordered strange metals: from conformal to hyperscaling-violating regimes*, *Nucl. Phys.* **B 892** (2015) 239 [arXiv:1411.3331] [INSPIRE].

[30] J.S. Steinhart and S.R. Hart, *Calibration curves for thermistors*, *Deep-Sea Research and Oceanographic Abstracts* **15** (1968) 497.

[31] B. Gouteraux and E. Kiritsis, *Quantum critical lines in holographic phases with (un)broken symmetry*, *JHEP* **04** (2013) 053 [arXiv:1212.2625] [INSPIRE].

[32] B. Goutéraux, *Universal scaling properties of extremal cohesive holographic phases*, *JHEP* **01** (2014) 080 [arXiv:1308.2084] [INSPIRE].

[33] A. Karch, *Conductivities for Hyperscaling Violating Geometries*, *JHEP* **06** (2014) 140 [arXiv:1405.2926] [INSPIRE].

[34] N. Iqbal and H. Liu, *Universality of the hydrodynamic limit in AdS/CFT and the membrane paradigm*, *Phys. Rev.* **D 79** (2009) 025023 [arXiv:0809.3808] [INSPIRE].

[35] M. Alishahiha, E. O Colgain and H. Yavartanoo, *Charged Black Branes with Hyperscaling Violating Factor*, *JHEP* **11** (2012) 137 [arXiv:1209.3946] [INSPIRE].

[36] S. Cremonini, M. Cvetic and I. Papadimitriou, in preparation.

[37] S. Cremonini, H.S. Liu, H. Lu and C.N. Pope, in preparation.

[38] R.A. Davison and B. Goutéraux, *Dissecting holographic conductivities*, *JHEP* **09** (2015) 090 [arXiv:1505.05092] [INSPIRE].

[39] M. Blake and A. Donos, *Quantum Critical Transport and the Hall Angle*, *Phys. Rev. Lett.* **114** (2015) 021601 [arXiv:1406.1659] [INSPIRE].

JHEP04(2017)009

[40] C.P. Herzog, P. Kovtun, S. Sachdev and D.T. Son, *Quantum critical transport, duality and M-theory*, *Phys. Rev.* **D 75** (2007) 085020 [hep-th/0701036] [INSPIRE].

[41] S.A. Hartnoll and A. Karch, *Scaling theory of the cuprate strange metals*, *Phys. Rev.* **B 91** (2015) 155126 [arXiv:1501.03165] [INSPIRE].

[42] S. Cremonini and L. Li, *Criteria For Superfluid Instabilities of Geometries with Hyperscaling Violation*, *JHEP* **11** (2016) 137 [arXiv:1606.02745] [INSPIRE].

[43] J. Bhattacharya, S. Cremonini and B. Goutéraux, *Intermediate scalings in holographic RG flows and conductivities*, *JHEP* **02** (2015) 035 [arXiv:1409.4797] [INSPIRE].

[44] M. Baggioli and O. Pujolàs, *Electron-Phonon Interactions, Metal-Insulator Transitions and Holographic Massive Gravity*, *Phys. Rev. Lett.* **114** (2015) 251602 [arXiv:1411.1003] [INSPIRE].

[45] A. Donos and J.P. Gauntlett, *Thermoelectric DC conductivities from black hole horizons*, *JHEP* **11** (2014) 081 [arXiv:1406.4742] [INSPIRE].

[46] J. Sonner, *On universality of charge transport in AdS/CFT*, *JHEP* **07** (2013) 145 [arXiv:1304.7774] [INSPIRE].

[47] W. Chemissany and I. Papadimitriou, *Lifshitz holography: The whole shebang*, *JHEP* **01** (2015) 052 [arXiv:1408.0795] [INSPIRE].

[48] I. Papadimitriou, *Hyperscaling violating Lifshitz holography*, *Nucl. Part. Phys. Proc.* **273-275** (2016) 1487 [arXiv:1411.0312] [INSPIRE].

[49] E. Kiritsis and Y. Matsuo, *Charge-hyperscaling violating Lifshitz hydrodynamics from black-holes*, *JHEP* **12** (2015) 076 [arXiv:1508.02494] [INSPIRE].

JHEP04(2017)009